

TECHNICAL NOTE

ON THE MODELLING OF LONG BONES IN STRUCTURAL ANALYSES*

Abstract—Results of experimental strain gauge and theoretical stress analysis methods are used to investigate the mechanical behavior of the human femur as a structural element under loading. It is shown that when the cortical bone material is assumed to demonstrate linear elastic, homogeneous and transversely isotropic behavior excellent agreement between experimental results and theoretical predictions is obtained. It also follows that the bone shaft can, by reasonable approximation, be represented by an axisymmetric model.

INTRODUCTION

A large number of investigations have been published with respect to the mechanical behavior of long bones, especially the human femur, recently as well as in the more distant past. A variety of experimental techniques (stress coating, extensometers, photoelastic models, strain gauges) and theoretical methods (beam theory, two and three-dimensional finite element methods, FEM) have been applied to determine stress and deformation patterns in the bone under various loading conditions. These efforts, not all of which are to be reviewed in this note, have contributed tremendously to a better understanding of the functional morphology of long bones, the distribution of stresses under various loading conditions, and their structural strength. Few investigators, however, have addressed the questions of modelling accuracy.

Scholten (1975) compared results of 2-D, 3-D FEM and beam theory analyses of a human femur in detail, concluding that good agreement is obtained for stresses in the femoral shaft up to the subtrochanteric region. Piziali *et al.* (1976) addressed several aspects of structural long-bone modelling, comparing results of different analytical and FEM models and evaluating the differences in results for several modelling approaches. Valliappan *et al.* (1977) roughly compared results of 2-D FEM, beam theory and experimental stress-coat analyses to find good agreement between results in a relative sense. However, the only precise and well-defined comparison between theoretical and experimental results of which this author is aware was published by Rohlmann *et al.* (1980). They studied a loaded cadaveric femur using both strain gauge techniques and FEM to evaluate stresses, finding reasonable relative but poor absolute agreement between results of both methods.

The objective of this note is to evaluate in some more detail the differences in results between experimental techniques and theoretical methods in analyzing the femoral diaphysis. This evaluation is based on findings from experimental strain-rosette measurements on the one hand and results from 3-D beam theory and FEM (torsion) analysis on the other (Huiskes *et al.*, 1976, 1981). By comparing results of different experimental and theoretical methods, the effects of material and geometrical modelling aspects are estimated and the accuracy of different modelling options established.

METHODS

The left femur of a 51-year-old male was embalmed with formaline, fixed into a laboratory setting, and the diaphysis

was applied with 100 strain-gauge rosettes with three elements each in a rectangular configuration. Element strains were measured while various loads were applied in turns to the femoral head (Fig. 1). The measured strains were used to calculate principal strains (ϵ_1, ϵ_2) and principal strain orientations (ϕ) according to Fig. 2. From these, the strains in the principal material directions ($\epsilon_1, \epsilon_2, \gamma_{12}$) were calculated. Then, assuming anisotropic (transversely isotropic) bone properties, as proposed by Carter (1978) based on data from Reilly and Burstein (1975), the stresses in the principal material directions were calculated from:

$$\begin{bmatrix} \sigma_1 \\ \sigma_2 \\ \tau_{12} \end{bmatrix} = \begin{bmatrix} S_{11} & S_{12} & 0 \\ S_{12} & S_{22} & 0 \\ 0 & 0 & S_{33} \end{bmatrix} \begin{bmatrix} \epsilon_1 \\ \epsilon_2 \\ \gamma_{12} \end{bmatrix}$$

with $S_{11} = E_{11}/(1 - \nu_{12}\nu_{21})$, $S_{22} = E_{22}/(1 - \nu_{12}\nu_{21})$, $S_{12} = E_{11}\nu_{21}/(1 - \nu_{12}\nu_{21})$, and $S_{33} = G_{12}$, where the longitudinal Young's modulus E_{11} was taken as 20,000 MPa, and:

$$\begin{aligned} \text{the transverse Young's modulus} & E_{22} = 0.68 E_{11} \\ \text{the shear modulus} & G_{12} = 0.19 E_{11} \\ \text{the Poisson's ratios} & \nu_{12} = 0.46 \text{ and} \\ & \nu_{21} = 0.31. \end{aligned}$$

To study the effects of these anisotropic (transversely isotropic) assumptions, stresses were also calculated by assuming isotropic properties. In this case, Young's modulus was taken as 20,000 MPa and Poisson's ratio as 0.37.

The right femur of the same cadaver was embedded in Araldite and sliced. The bone contours in each section were digitized and cross-sectional properties calculated (areas, moments of inertia, principal inertia axes). An approximate axisymmetric cross section with inner radius r and outer radius R was determined for each section as well, in such a way that both the areas and the polar moments of inertia of the real sections were reproduced.

Using the cross-sectional data, longitudinal direct stresses due to bending and axial loading were calculated by applying 3-D beam theory in the real section, as well as in the axisymmetric approximation. Results were compared with corresponding experimental findings.

Shear stresses in the cross section due to torsion were calculated in two ways. By using the axisymmetric geometry, the maximal shear stresses at the bone surface were approximated by

$$\tau = \frac{M_z R}{J} \text{ (MPa)}$$

* Received 12 February 1981; in revised form 3 August 1981.

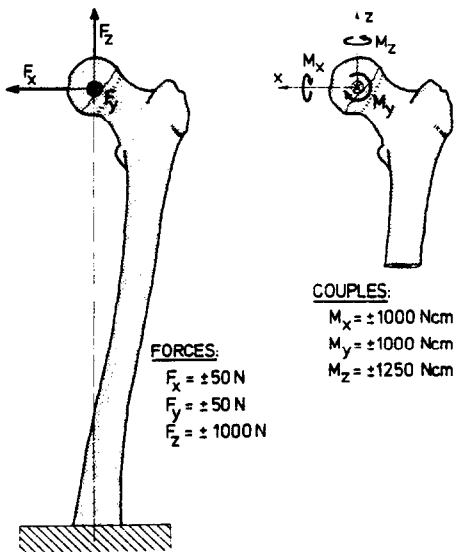


Fig. 1. Forces and couples applied to the femoral head in turns. The loads were applied in positive, as well as negative, orientation.

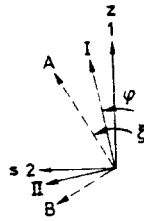


Fig. 2. A local coordinate system for a strain-gauge rosette. The longitudinal material directions are indicated by axis 1 (= z-axis, longitudinal bone axis) and by axis 2 (= s-axis, tangential bone axis). Principal strain orientations: I, II; principal stress orientations: A, B.

where M_z is the torque (Nmm), R the outer radius (mm), and J the polar moment of inertia (mm^4).

In addition, the torsional shear stresses in the real section were calculated by using Saint Venant's warping theory. The elliptical differential equation describing the stress function in the cross section and its boundary conditions were solved using a FEM program for this purpose. Again, results were compared to those of the corresponding experimental findings.

RESULTS

The experimental results showed that the bone material behaved in a linear elastic manner by comparing strains measured for positive and negative pure bending couples (up to 12,500 Nmm) on the femoral head. Differences in absolute strain values showed to be less than 2 per cent in this comparison. Immediately after load application, some viscoelastic behavior was apparent which diminished completely within three minutes. It should be mentioned here that when forces in the longitudinal bone direction are applied on the

head, geometrically nonlinear behavior results (Huiskes *et al.*, 1981) due to an additional moment on the head brought forward by a significant lateral displacement.

The discussion of results focuses on one section as an example, shown in Fig. 3. The strain-gauge rosettes 38–44 (of which No. 41 failed in the course of time), the local coordinate system (x' , y'), and the axisymmetric approximation (R , r) are indicated in this figure. Properties of this cross section are shown in Table 1. (The principal axis orientation angle α is measured clockwise between the x' -axis and the maximal inertia axis.)

Figures 4 and 5 show comparisons of stresses in the principal material coordinate system (σ_1 , σ_2 and τ_{12}) for pure bending couples around the y' and x' axes respectively. Experimental results are shown evaluated with both the isotropic and anisotropic (transversely isotropic) assumptions, compared to stresses computed with 3-D beam theory, for the real section as well as for the axisymmetric approximation.

Figure 6 shows a comparison of stresses in the principal material coordinate system (τ_{12} , σ_1 , σ_2) due to torsion. Here, too, experimental results are shown evaluated with the isotropic and anisotropic (transversely isotropic) assumptions, as well as shear stresses calculated with the Saint Venant theory and by using the axisymmetric approximation.

DISCUSSION AND CONCLUSIONS

Apparently there is only a slight difference between the most significant stress components due to bending calculated from the measured strains using the isotropic assumptions as compared to using the transversely isotropic data. This

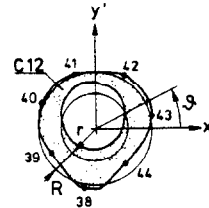


Fig. 3. Section C12 is shown with the corresponding rosettes 38 through 44, local coordinate system (x' , medial to lateral; y' , posterior to anterior), and the axisymmetric approximation. Angle θ defines a point on the bone surface.

Table 1. Cross-sectional properties of section C12, as calculated from its digitized bone contours, and properties of its axisymmetric approximation (area (A) and polar moment of inertia (J) are identical for both)

| Property | Symbol | Units | Value |
|----------------------------------|-------------------|---------------|-------|
| Area | A | mm^2 | 4.37 |
| Max. area moment of inertia | I_{\max} | mm^4 | 3.49 |
| Min. area moment of inertia | I_{\min} | mm^4 | 2.81 |
| Polar moment of inertia | J | mm^4 | 6.30 |
| Inertia axis orientation | α | deg. | 49.6 |
| Outer radius | R | mm | 14.60 |
| Inner radius | r | mm | 8.63 |
| Moment of inertia axisymm. appr. | I_{appr} | mm^4 | 3.13 |

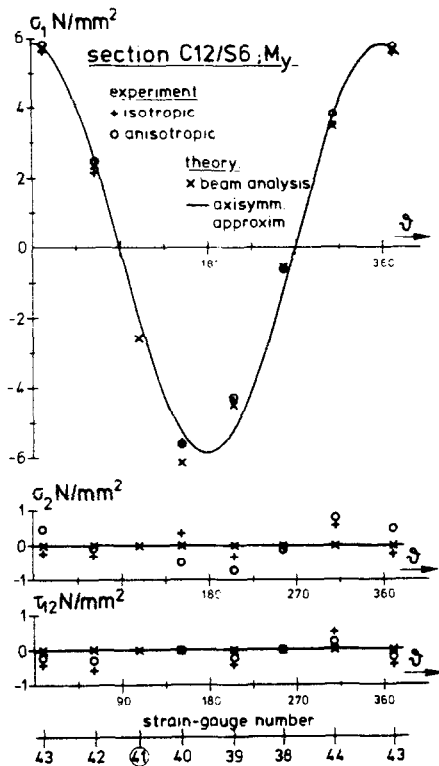


Fig. 4. Comparison between experimental and theoretical stresses in the principal material coordinate system at the bone surface, due to loading by a bending couple $M_y' = -12,500$ Nmm, as functions of θ (rosette No. 41 failed).

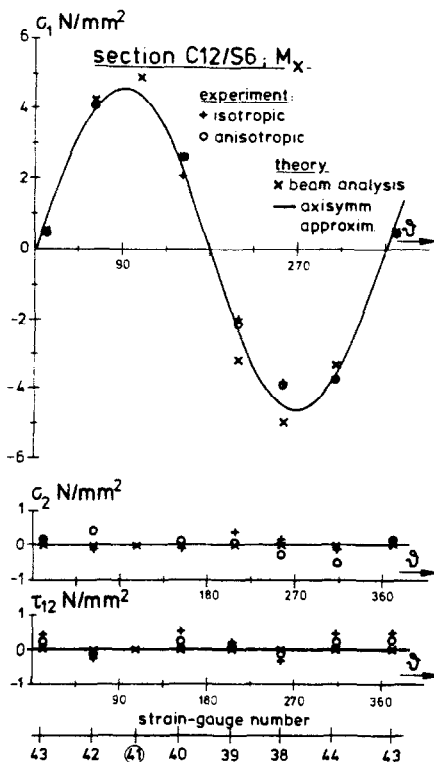


Fig. 5. Comparison between experimental and theoretical stresses in the principal material coordinate system at the bone surface, due to loading by a bending couple $M_x' = 10,000$ Nmm, as functions of θ (rosette No. 41 failed).

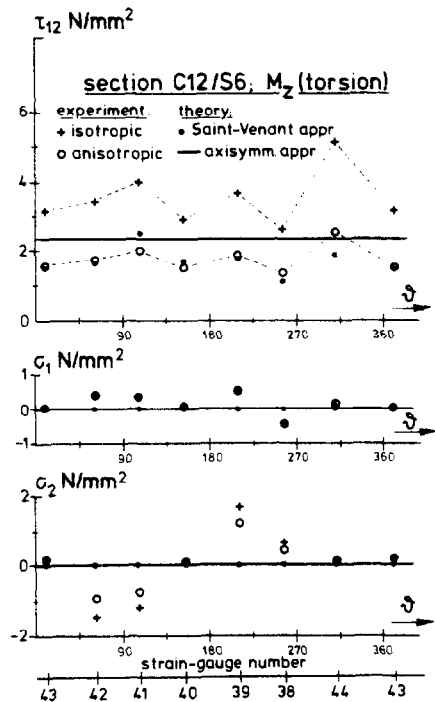


Fig. 6. Comparison between experimental and theoretical stresses in the principal material coordinate system at the bone surface, due to loading by a torque $M_z = 10,000$ Nmm, as functions of θ .

seemingly contradicts conclusions expressed by Carter (1978) that there should be a significant difference. However, this is not surprising because these stress components are in the longitudinal bone direction in which the Young's modulus was taken as 20,000 MPa in both cases. Carter (1978), on the other hand, chose an average of the longitudinal and transverse moduli for his isotropic analysis. His conclusions fully apply to other than the longitudinal stress components in bending (and, as to that, axial loading) and to stresses due to torsion (Fig. 6).

In both the application of beam analysis and Saint Venant's theory, the calculated stresses are independent from the elastic constants. Hence, the excellent agreements between the stresses calculated from the measured strains with the transversely isotropic assumptions on the one hand, and the stresses computed with beam (Figs. 4 and 5) and Saint Venant's theories (Fig. 6) on the other, reflect a good choice for the longitudinal Young's modulus and lend confidence to the applicability of the elastic constants calculated by Carter (1978) from data published by Reilly and Burstein (1975).

Van Buskirk and Ashman (1981) could not fully confirm the transverse isotropy reported by Reilly and Burstein (1975). The differences would not significantly affect the results for bending (Figs. 4 and 5), although small differences in σ_2 and τ_{12} could result. However, the agreement between experimental and Saint Venant results for torsion in the shear stresses (Fig. 6) would be far less satisfactory when the shear modulus found by Van Buskirk and Ashman (1981) was used.

A value of 20,000 MPa for the longitudinal modulus, as used here, is somewhat higher than usually given as average for human cortical bone in the literature (e.g. Evans, 1973; Reilly and Burstein, 1975; Van Buskirk and Ashman, 1981), but this no doubt reflects the effect of embalming. Evans (1973) showed that the stiffness of embalmed human cortical bone may increase up to 12% when compared to fresh bone. It should be remembered here that on the one hand embalming

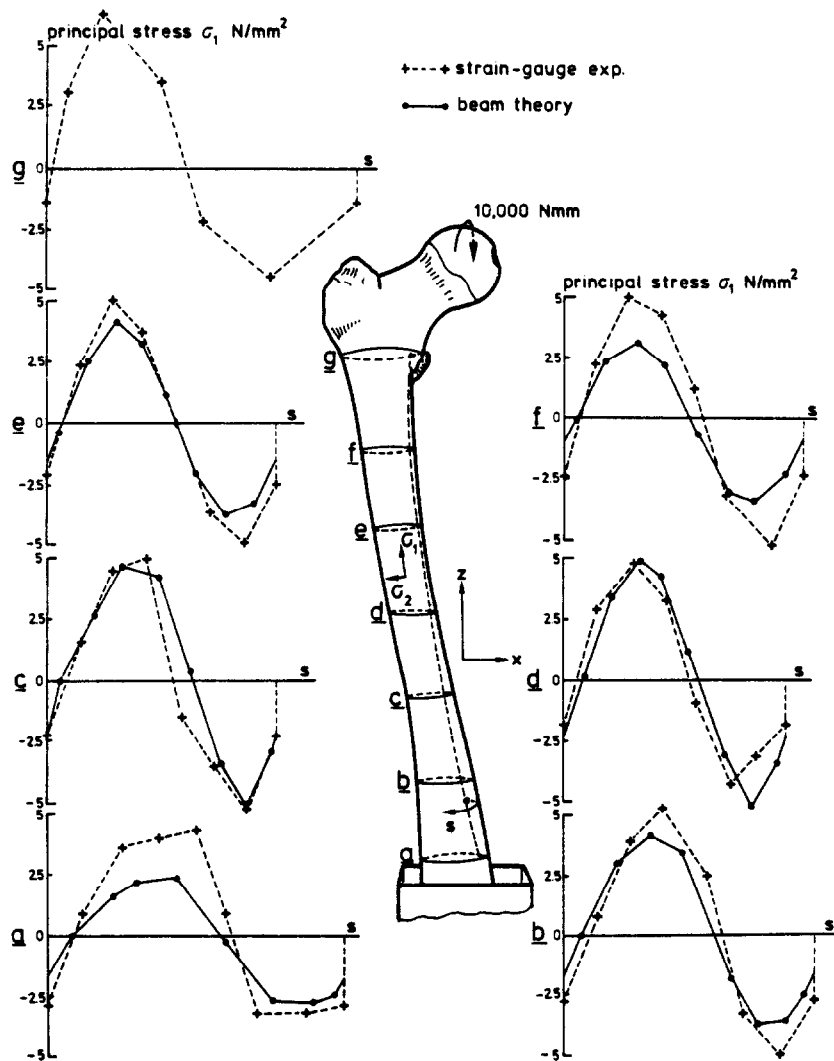


Fig. 7. A comparison of maximal principal stresses on several bone levels as evaluated from the strain measurements (isotropic assumption), and as calculated using 3-D beam theory, on loading with a bending moment around the x -axis. Discrepancies, apparent in this loading case especially, are due to local inhomogeneities.

was necessary in this case to allow for the bone to retain its properties during the long test period, while on the other it keeps the rosettes from loosening and the strain values from drifting, occurring in fresh bone caused by local dehydration effects.

It is apparent from Fig. 6 that when isotropic assumptions are used to evaluate the shear stresses from the experimental strains, these far exceed the theoretical predictions. Good agreement with the Saint Venant theory is found when using the transversely isotropic assumptions, where the shear modulus (G_{12}) is about half the isotropic value. The prediction of the axisymmetric approximation is not bad in a relative sense. Piziali *et al.* (1976) found in their theoretical analysis of the tibia a 75% underestimation of the maximal shear stresses when using the circular geometry, when compared to the results of Saint Venant's theory applied to the real section. Here, an overestimation of about the same magnitude is apparent. Since both theoretical methods give shear stresses independent of the elastic constants when the torque is prescribed, the cause for this discrepancy is not

obvious. A probable explanation lies in the differences between the femoral and the tibial geometries; the latter having a much thinner cortex. Figure 6 shows some discrepancies in experimental results and theoretical predictions with respect to the direct stress σ_2 , the cause for which is unclear.

When transverse forces are applied to the femur (F_x , F_y , compare Fig. 1), shear stresses will occur in the cross sections as well. The principal strain orientations, however, do not differ significantly from those in the case of bending by pure couples if far enough away from the load. Hence, the deformations are principally in the bending mode, as was also concluded by Piziali *et al.* (1976). For the transverse-load values used here (50 N), the experimental shear stresses were up to about 10% of those found for torsion (transversely isotropic assumption).

The stresses calculated by using beam theory for the axisymmetric shape in bending approximate the experimental results surprisingly well. The prediction of shear stresses due to torsion is not so satisfactory, but still acceptable for an

approximate analysis. When the bone cross section has a more elliptical shape, as compared to an axisymmetric shape, the approximation, of course, is not so good but differences in experimental and theoretical results are still reasonably small (Huiskes *et al.*, 1981).

The cross section of the bone evaluated here is a typical one for the mid-diaphysis. Other cross sections give comparable results. However, minor inhomogeneities occur throughout the bone, the effects of which become apparent mainly in the non-physiological loading cases. Figure 7, for instance, shows a comparison between maximal principal stresses as evaluated from the strain measurements (isotropic assumptions), and as calculated using beam theory for a bending moment around the x-axis. The agreement (especially on levels *g* and *f*) is far less than in the case of the more physiological loading case of bending around the y-axis. This points to a lower value of the longitudinal modulus, locally in the anterior and posterior cortex, where in natural circumstances the stresses do not reach very high values.

It can be concluded from these results that when assuming the cortical bone material to exhibit linear elastic, homogeneous and transversely isotropic behavior an excellent agreement between theoretical and experimental results can be obtained, although some local inaccuracies due to non-homogeneity should be expected. Since these requirements can be easily met with finite element analysis, the accuracy of an FE model would only depend on an adequate mesh refinement.

However, when torsion is not considered and only the most significant (longitudinal) stress components are of interest, a good approximation can be obtained from assuming the cortical bone to be isotropic. In this case, three-dimensional beam theory has better opportunities as a method of analysis compared to FEM in view of complexity, cost efficiency, and potential accuracy. In addition, a reasonable approximation of the bone shaft stresses can be obtained by assuming the bone to be axisymmetric.

Acknowledgements—The data on which these results are based were obtained from a number of research projects involving several students, technicians and scientists of the Division of Applied Mechanics, Eindhoven University of Technology, The Netherlands.

The final efforts of this project were carried out at the Biomechanics Laboratory, Department of Orthopedics, Mayo Clinic, Rochester, MN, USA, where the author was

supported by a grant from The Netherlands Organization for the Advancement of Pure Research.

*Orthopaedic Biomechanics Lab,
University of Nijmegen,
6500 HB Nijmegen,
The Netherlands*

R. HUISKES

REFERENCES

- Carter, D. R. (1978) Anisotropic analysis of strain rosette information from cortical bone. *J. Biomechanics* 11, 199–202.
- Evans, F. G. (1973) *Mechanical Properties of Bone*. Charles C. Thomas, Springfield, IL.
- Huiskes, R., Heugten, P. C. M. V. and Slooff, T. J. (1976) Strain-gauge measurements on a loaded femur, intact as well as provided with prostheses. *Proc. of the 29th ACEMB*, Boston, MA.
- Huiskes, R., Janssen, J. D. and Slooff, T. J. (1981) A detailed comparison of experimental and theoretical stress analyses of a human femur. In: *Mechanical Properties of Bone*, AMD—Vol. 45 (Edited by Cowin, S.) pp. 211–234. Am. Soc. of Mech. Engr., New York.
- Piziali, R. L., Hight, T. K. and Nagel, D. A. (1976) An extended structural analysis of long bones, application to the human tibia. *J. Biomechanics* 9, 695–701.
- Reilly, D. T. and Burstein, A. H. (1975) The elastic and ultimate properties of compact bone tissue. *J. Biomechanics* 8, 393–405.
- Rohmann, A., Bergmann, G. and Köbel, R. (1980) The relevance of stress computation in the femur with and without endoprostheses. *Int. Conf. Proceedings, Finite Elements in Biomechanics*, Vol. 2 (Edited by Simon, B. R.) pp. 549–567. The Univ. of Arizona, Tucson, AZ.
- Scholten, R. (1975) Ueber die Berechnung der mechanische Beanspruchung in Knochenstrukturen mittels für den Flugzeugbau entwickelte Rechenverfahren. *Med. Orthop. Technik* 6, 130–138.
- Valliappan, S., Svensson, N. L. and Wood, R. D. (1977) Three-dimensional stress analysis of the human femur. *Comput. Biol. Med.* 7, 253–264.
- Van Buskirk, W. C. and Ashman, R. B. (1981) The elastic moduli of bone. In: *Mechanical Properties of Bone*, AMD—Vol. 45 (Edited by Cowin, S.) pp. 131–143. Am. Soc. of Mech. Engr., New York.